Highlights

-Porous hydrogel microspheres were synthesised and mixed with dry-water forming a colloidal system

-Formation of methane gas hydrates in the colloidal system was fast and high in hydration capacity

-The system is reusable for methane storage

Reversible Methane Storage in Porous Hydrogel Supported Clathrates

Ailin Ding[1], Liang Yang[2], Shuanshi Fan[2]*, Xia Lou[1]*

[1]*Department of Chemical Engineering, Curtin University, Kent Street, Western Australia 6102, Australia.*

[2]*Key Lab of Enhanced Heat Transfer and Energy Conservation, Ministry of Education, School of Chemistry and Chemical Engineering, South China University of Technology, Guangzhou 510640, China*

*Corresponding authors:
Xia Lou. Tel.: +61 9266 1682; Fax: +61 9266 2681; Email: X.Lou@curtin.edu.au.
Shuanshi Fan. Tel.: +86 20 22236581; Fax: +86 20 22236581; Email: ssfan@scut.edu.cn.

Abstract

Methane gas hydrates are a promising alternative for storage and transport of natural gas. In this paper, porous poly(2-hydroxyethyl methacrylate) (PHEMA) and poly(2-hydroxyethyl methacrylate-co-methacrylic acid) (PHEMA-co-MAA) hydrogel microspheres were synthesised and examined as a reusable scaffold for methane storage in the hydrated form. The hydration kinetics, methane storage capacity of the hydrogel microspheres and a mixed colloidal system made of hydrogel particles and dry-water droplets were investigated in a 300 cm^3 steel vessel at 273.2 K and varying pressures. Hydration of methane in the mixed colloidal system is high in capacity and exceedingly reversible. Higher pressure and smaller size of hydrogel microspheres result in higher capacity and kinetics, however reduce recyclability of the hydration. The porous hydrogel particles alone are too soft for reuse and need to be improved for practical application.

Keywords: Methane gas hydrate; natural gas clathrate; methane storage; hydrate formation kinetics; porous hydrogels.

1. Introduction

Gas hydrates are ice-like clathrate compounds consisting of a host lattice formed by hydrogen-bonded water molecules and a large variety of small guest molecules enclosed in the lattice. They form when small gas molecules including methane, carbon dioxide and hydrogen, come into contact with water at low temperature and high pressure (Sloan and Koh, 2008; Koh, 2002). It is generally accepted that the formation of gas hydrates is a gas-liquid or gas-solid interfacial phenomenon. The formation kinetics of gas hydrates is largely dependent on the nucleation and growth rate of the gas hydrates, the rate of methane transfer through the liquid or solid phase, and the rate of heat transfer.

Methane hydrate has a relatively high gas to solid ratio, storing up to 180 volume of gas (at standard conditions) in 1 volume of hydrate (Sloan, 2003) and can be held in a metastable solid state at atmospheric pressure (Stern et al., 2001). These make methane hydrates a promising alternative for storage and transport of natural gas (Gudmundsson and Graff 2003; Mori 2003; Masoudi and Tohidi, 2005). However, the application of the technology has been challenged by the slow formation rate and low storage capacity, as well as the thermal stability of methane hydrates.

Common methods for increasing clathrate forming kinetics include the use of high pressures, vigorous mechanical mixing, chemical additives and micron sized ground ice particle (Sloan, 2003). Among the chemical additives, surfactants has been found to promote gas hydrate formation without affecting the thermodynamics of hydrate crystallization (Zhong and Rogers, 2000; Yoslim et al., 2010; Okutani et al., 2008). Tetrahydrofuran (THF) (Giavarini, 2008), cyclopentane (Sun et al., 2003; Zhang et al.,

2004), and tetra-*iso*-amylammoinium bromide(TiAAB) (Wang et al., 2009) have also been used as hydrates promoters. The added promoter occupies some of the cavities in the clathrate structure, therefore reducing the volume available for the trapping of gas molecules (Carter et al., 2010). More recent work by Cooper's group has been focused on high surface area polymers and dry-water. The latter are made of free-flowing water droplets surrounded by hydrophobic silica nanoparticles that prevent droplet coalescence (Binks and Murakami, 2006). For example, polystyrene-based polyHIPE (high internal phase emulsion) (Su et al., 2008), a foamed polyurethane (Talyzin 2008) and a slightly cross-linked poly(acrylic acid) sodium salt (PSA) (Su et al., 2009) have been used to increase the storage capacity of hydrogen in THF-stabilized clathrates. However, using same materials as a support media for methane storage was less successful. TiAAB semi-clathrates were used with PolyHIPE for reversible methane storage. Up to 20 charge-discharge cycles were accomplished. However, only 35-40 v/v storage capacity was achieved (Wang et al., 2009). The low methane storage capacity was assumed due to the hydrophobicity of the polymer and its poor water wettability. Using dry water by the same group, a much higher methane storage capacity (175 v/v) and a relatively rapid formation rate of methane hydrates was achieved (Wang et al., 2008). The authors expanded their work and utilised a gelling agent to form 'dry gel' so as to stabilise the dry system toward coalescence, therefore improving the recyclability of the material. One of the reported 'dry gel' systems was found to be recyclable over eight heating/cooling cycles with a gas capacity of 130 v/v (Carter et al., 2010). Inspired by the work of Cooper's group, we investigated the possibility of utilisation of cross-linked three dimensional porous poly(2-hydroxyethyl methacrylate) (PHEMA) hydrogel microspheres as support for methane hydrate formation.

PHEMA polymers are often produced by free radical polymerisation of hydroxyethyl methacrylate (HEMA) in the presence of a cross-linker and an initiator. When in contact with water, PHEMA polymers absorb and retain large amounts of water becoming hydrogels. These hydrogels maintain a transparent and homogenous network that is suitable for such applications as contact lens and intraocular lens in which optical clarity and limited diffusional characteristics are required. When PHEMA hydrogels are produced in the presence of porogens or a large amount of water, phase separation occurs as a consequence of thermodynamic interactions between water and polymer network, leading to the formation of a spongy and opaque hydrogel containing interconnected pores much greater than those in the homogenous hydrogels (Lou et al., 2004). These hydrogels have been found useful in the development of ophthalmic implants and controlled drug delivery systems (Chirila et al., 1998; Hicks et al., 2006; Lou et al., 2007; Wang et al., 2010). The high water content, excellent hydrophilicity and interconnected pores of these hydrogels could be ideal to support the methane hydrate formation and to enhance gas permeation and interactions with water molecules. In this work, porous microspheres of PHEMA and a copolymer of HEMA with methacrylic acid (MAA), PHEMA-co-MAA, were produced by a suspension polymerization in the presence of a porogenic mixture of cyclohexanol and 1-octanol (Horak et al., 1993). The produced porous PHEMA spherical hydrogels were examined, alone and together dry-water, for reversible methane storage. The hydrate formation kinetics and capacity, and the reusability of these hydrogels were investigated.

2. Experimental

2.1 Materials

2-Hydroxyethyl methacrylate (HEMA) and ethyleneglycol dimethacrylate (EDMA) were supplied by Bimax. 2.2'-Azobis(2-methylpropinitrile) (AIBN) was purchased from Sigma-Aldrich and recrystallized from ethanol prior to use. Cyclohexanol (99%) was purchased from APS Chemicals. Other chemicals including 1-octanol (99 %), poly(N-vinyl-2-pyrrolidone) (PVP, MW=360,000), and methacrylic acid (MAA, 99%) were purchased from Sigma-Aldrich and used as received.

2.2 Preparation and characterisation of hydrogel microspheres

The following procedure was used to prepare the hydrogel microspheres: to a 15 ml of porogen mixture (organic phase) containing 1-octanol and cyclohexanol of 2:3 volume ratio, 9.5 ml of monomer (HEMA or HEMA-MAA at a volume ratio of 8.5:1), 0.1 g of initiator (AIBN), and 0.5 ml of crosslinking agent (EDMA) were added and well mixed. The organic phase was then mixed with 75 ml of a 1% PVP aqueous solution in a glass flask and then purged with nitrogen for 30 min. The polymerization was carried out at 70°C for 8 h with continuous stirring at 180 rpm. After cooling to room temperature, the polymer particles were washed with water, methanol and water successively. The hydrogel particles were suspended in water for storage (Figure 1a). Soft hydrogel particles (Figure 1b) after the removal of free water from the suspension were used for further investigation.

SEM images of hydrogel microspheres were taken on a Philips XL 30. The necessary conductivity was guaranteed through a gold coating which was applied through physical vapour deposition (PVD). All hydrogel microspheres were freeze-dried prior to the SEM examination. Light microscopy images of the dried microspheres were

obtained using a Nokon Optiphot-2 with a Pulnix digital camera. The ζ-potential of the microspheres was measured using a Malvern Zetasizer Nano-ZS and folded capillary cells (DTS 1060 from Malvern Instrument).

Figure 1 Photos of (a) water suspension of hydrogel particles, (b) free hydrogel particles, and (c) mixed hydrogel particles with dry-water.

2.3 Preparation of mixed dry-water and hydrogel particles

Mixed dry-water and hydrogel particles were produced using the method reported by Carter et al. (2010). In brief: dried hydrogel microspheres (2.00 g) were mixed with HB630 (1.00g) and then hydrated in deionized water (17.00 g) in a blender (Philips HR1727/06, 1.5 litre). Mixing was carried out at a speed of 18000 rpm for 3 x 15 seconds at ambient conditions. Free flowing particles containing hydrogels mixed with silica nanoparticles were produced (Figure 1c).

2.4 Synthesis of methane hydrates

Synthesis of methane hydrates was carried out using a method similar to that was reported in a previous paper (Yang et al., 2011). The experimental set-up is shown schematically in Figure 2. Before each experiment, a 300 cm^3 stainless steel high-pressure vessel (Jiangsu Hai'an Scientific Research Instrument Factory) was washed with deionized water and charged with 15.00g of hydrogel microspheres or the

mixture of hydrogel-dry water particles. The vessel was then flushed with methane (99.99 % purity, Guangzhou Yinglai Gases Co., Ltd) three times to remove air in the vessel. Afterwards, a circulating cooling bath (THD-3010, Zhejiang Ningbo Tianheng Instrument Factory) with a heating/cooling coil was turned on to adjust the vessel temperature to 273.2 K. Two thermal resistance detectors (Pt100, ± 0.01 K, 253 ~ 473K Jiangsu Plaza Premium Electric Instrument Co., Ltd.) were used to monitor the temperatures of gas and liquid phases in the reaction vessel. Once the desired temperature was reached and maintained constant for several minutes, methane was injected into the vessel until the given pressure was reached (4.5 or 7.5 ± 0.1 MPa). The pressure in the vessel was monitored using a pressure transducer (DG1300, 0~40 ± 0.01 MPa, Guangzhou Senex Instrument Co., Ltd.). The time (t), temperature (T) and pressure (P) was recorded at 10-second intervals with Agilent 34970A Data Logger (Agilent Technologies Co., Ltd.). The formation of methane hydrates was shown when the temperature increased due to the latent heat and the gas pressure decreased as a consequence of methane consumption. The hydration process was assumed to reach its completion when the pressure drop rate was less than 0.01 MPa over 30 min.

For the reversibility measurement, the formed hydrates were first dissociated by raising the system temperature back to 298.5 K, allowing full release of methane from the hydrates form. The vessel was then cooled to 273.2 K. This cycle was repeated for several times.

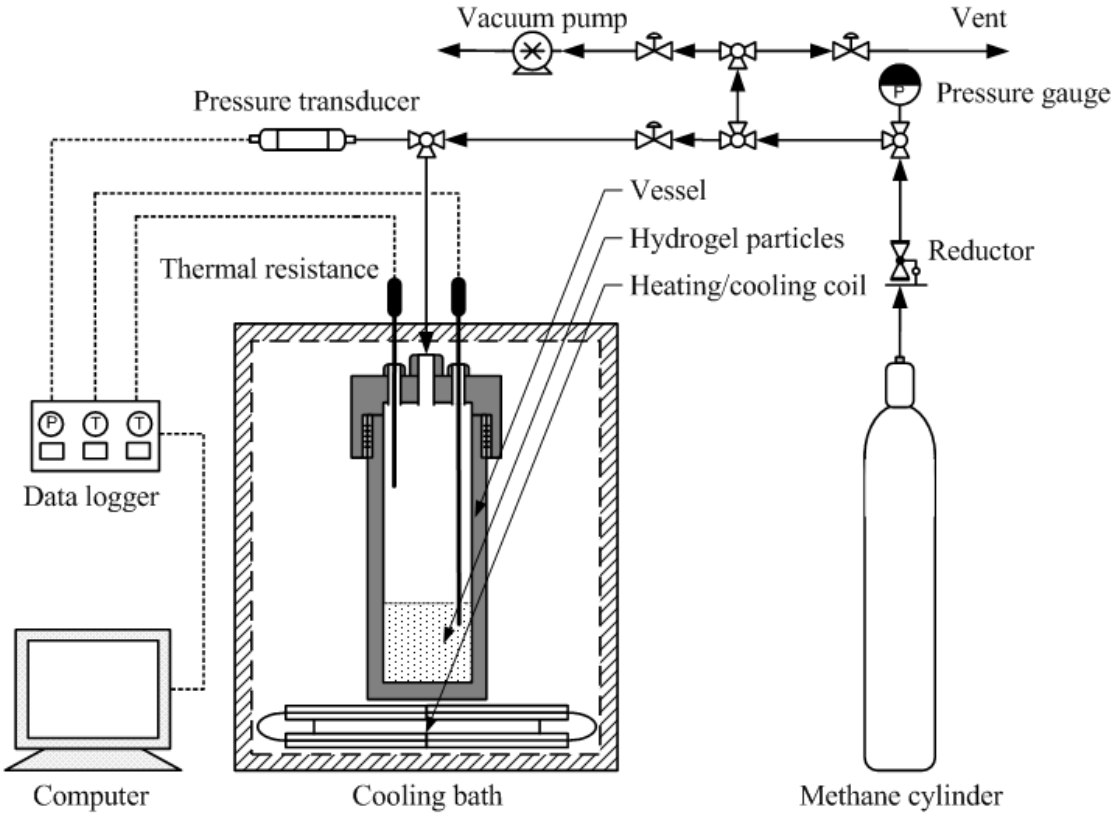

Figure 2 Schematic diagram of experimental set-up.

2.5 Determination of methane consumption

Methane consumption during the hydration process was determined from the pressure-temperature data and was used as an estimation of the storage capacity of methane in the hydrates form. The compressibility factor "*Z*" in real gas law (*PV* = *nZGT*) was utilized to calculate the number of moles (*n*) of free methane present in the vessel under each set of pressure-temperature (*P*-*T*) points, where *G* is universal gas constant. The compressibility factor can be computed by Redlich-Kwong equation (Redlich and Kwong, 1949). The free methane volume (*V*) was assumed constant throughout the reaction (i.e., volume changes due to phase transitions were neglected).

3. RESULTS AND DISCUSSION

3.1 Microsphere preparation and characterisation

Preparation of PHEMA microspheres by suspension polymerizing HEMA in an aqueous solution is a well-established process developed for chromatographic packing materials and artificial emboli (Horak et al., 2006). To obtain a macroporous structure, suspension copolymerization of HEMA and crosslinking agent EDMA is often carried out in the presence of porogens. Both low molecular weight porogens and polymeric porogens can be used to prepare PHEMA microspheres. In this work, low molecular weight porogens, cyclohexanol and 1-octanol, were used for the convenience of removal after polymerisation. The water-insoluble porogen 1-octanol was used to extract the hydrophilic monomers from water phase. Polymerisation took place in the organic phase in which 1-octanol is a poor solvent and cyclohexanol is a good solvent for the polymerised HEMA. Phase separation occurs within the organic phase due to the thermodynamic interaction between 1-octanol and polymer network, leading to the formation of porous structure. It is shown in Figure 3a-d that the produced PHEMA and PHEMA-co-MAA microsphere are in the range of tens to hundreds micrometres. Each microsphere consists of aggregated fine polymer particles (~1μm) that are divided by the interconnected pores and channels (Figure 3e and f). The size of polymer particles and pores were dependant on the polymerisation condition and the amount of 1-octanol in the oil phase. The microspheres were divided into two portions, < 100 μm and > 100 μm, for methane storage investigations. The measured ζ-potential was -10.4 ± 0.59 mV for PHEMA and -23.1 ± 0.95 mV for PHEMA-co-MAA.

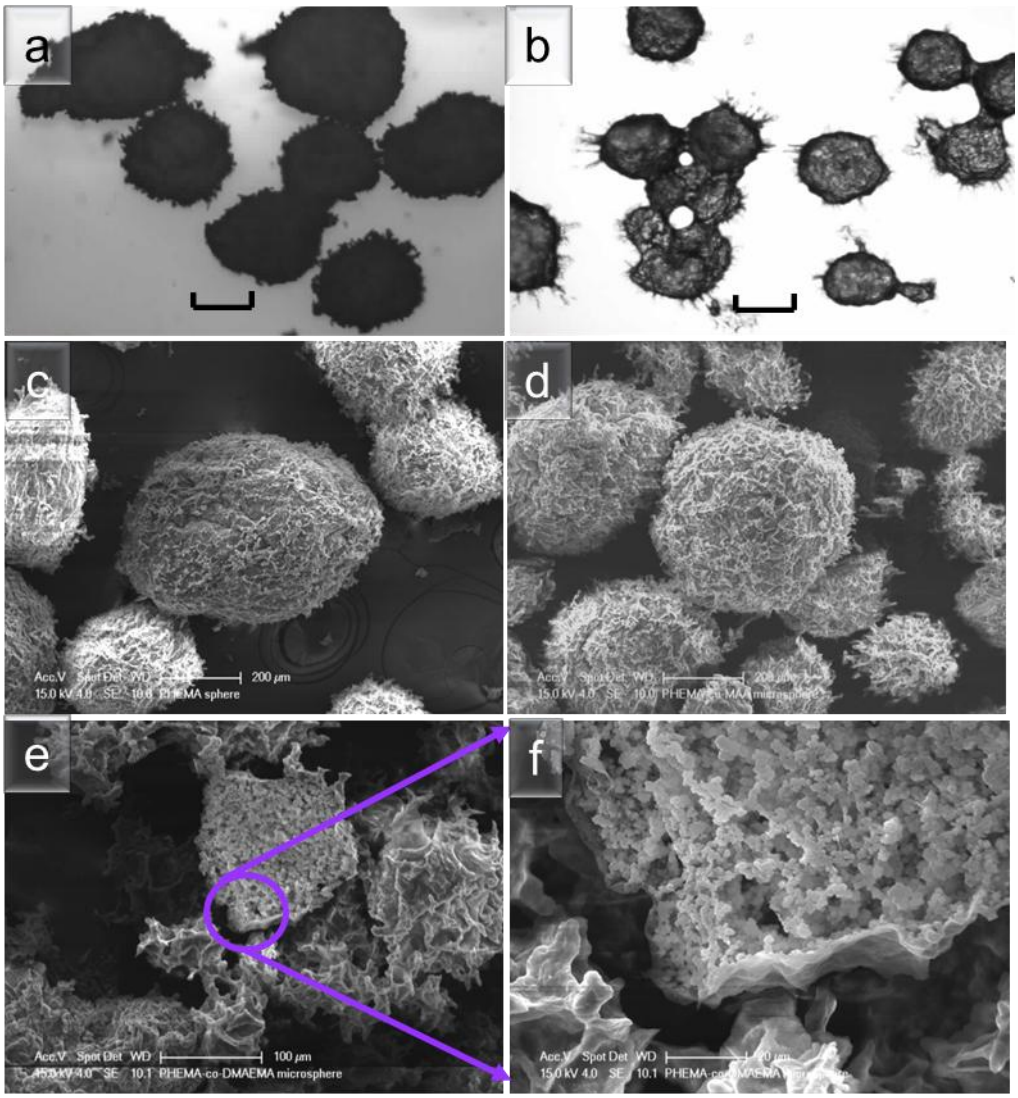

Figure 3 Light microscopic and SEM images showing the size of PHEMA (a, c) and PHEMA-co-MAA (b, e) microspheres, and the interconnected pores and channels (f, g) within the hydrogel microspheres. In a and b, magnification bar = 200 µm.

3.2 Formation of methane hydrates

Formation of methane hydrates in various systems was revealed by the T-P-t plots displayed in Figure 4. In the presence of dry water, or the mixtures of dry water with PHEMA (<100 μm), PHEMA-co-MAA (<100 μm) and PHAME-co-MAA (>100 μm), a rapid decrease in pressure, accompanied by an increase in temperature was observed within the first 2-3 hours, indicating the formation of methane hydrates. The pressure reached a plateau at around 400 min, demonstrating the completion of most hydrate growth. The increase in temperature in this time period is a result of the exothermal process of methane hydrates formation. For pure PHEMA hydrogels microspheres, no significant change in either the pressure or temperature was observed, indicating that little hydrates were formed. The particles were examined under an optical microscope after the hydration experiment. They were found attaching to each other forming a 'paste' of hydrogel particles, therefore preventing the fast and large volume formation of hydrates. Increased ζ-potential in PHEMA-co-MAA microspheres did not prevent the adhesive effect of the hydrogel particles. Methods of improving the anti-adhesiveness of the hydrogel particles are under investigation.

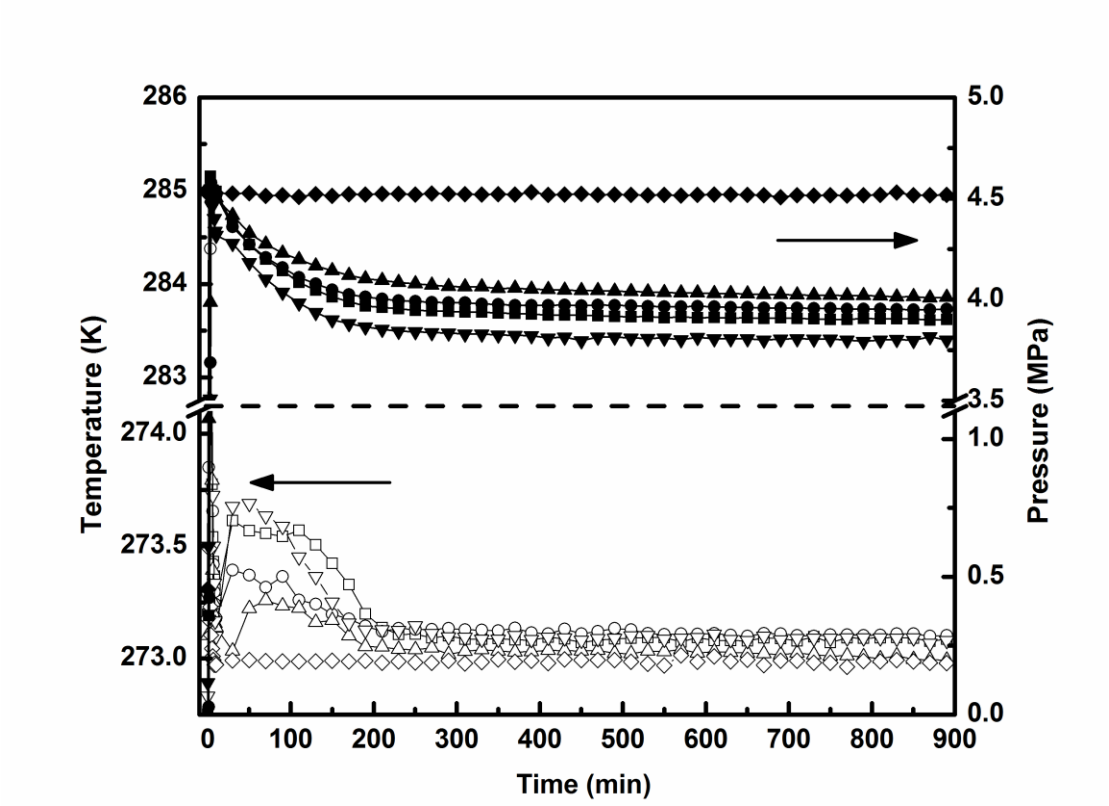

Figure 4 Temperature and pressure history in one methane storage cycle showing (1) the rapid formation of methane hydrates in: dry water (▿&▼), dry water + PHEMA (<100 μm) (□&■); dry water + PHEMA-co-MAA (<100 μm) (○&●); dry water + PHEMA-co-MAA (>100 μm) (△&▲), and no formation in pure PHEMA (◇◆). Operation conditions: T=273.2 K, P= 4.5 MPa.

3.3 Methane storage capacity, kinetics and reversibility

The pressure change was used to calculate methane consumption during the hydrates formation as described in the experimental section. The results were displayed in Figure 5, in which the volume of methane consumed by per gram of added water in the reaction vessel was used as a measure of the methane storage capacity in various systems. At 4.5 MPa, the calculated methane storage (after 900 min) was 160 cm^3/g, 154 cm^3/g, 142 cm^3/g for dry-water, and the mixed PHEMA (<100μm) and PHEMA-co-MAA (<100 μm) with dry-water respectively, showing a slight reduction of methane capacity after mixing these hydrogel particles with dry water. A more significant reduction, to 123 cm^3/g, was observed when the larger particles of

PHEMA-co-MAA (> 100 μm) were used. This is due to the reduced surface area for methane to transport and interact with the water molecules. When a higher initial pressure (7.5 MPa) was employed in the experiment, the methane capacity in PHEMA-co-MAA (>100 μm) increased to 144 cm^3/g, due to the enhanced gas diffusion with increased pressure. These results demonstrate that the smaller size of hydrogel particles and higher operational pressure lead to greater methane storage capacity. Repeated experiments on pure hydrogel microspheres showed a low storage capacity in the range of 20 to 70 cm^3/g. These results were not as reproducible as the results obtained from dry-water and the mixed dry-water and hydrogel systems.

The linear fittings of the methane consumption curves during the rapid hydration time period were carried out to determine the maximum formation rate of hydrates (Karaaslan and Parlaktuna, 2000; Lee et al., 2007). It can be seen from these fittings (Figure 5) that methane consumption was much quicker at 7.5 MPa. When the pressure was reduced to 4.5 MPa, methane hydrates formation was quicker in dry-water and the smaller microspheres made of PHEMA or PHEMA-co-MAA (< 100 μm) than in the larger PHEMA-co-MAA (>100 μm) microspheres. The estimated time at which 90% methane was consumed, t_{90}, for each system was listed in Table 1. The results again demonstrate that the smaller particle size and higher pressure are benefit to the formation of methane hydrates.

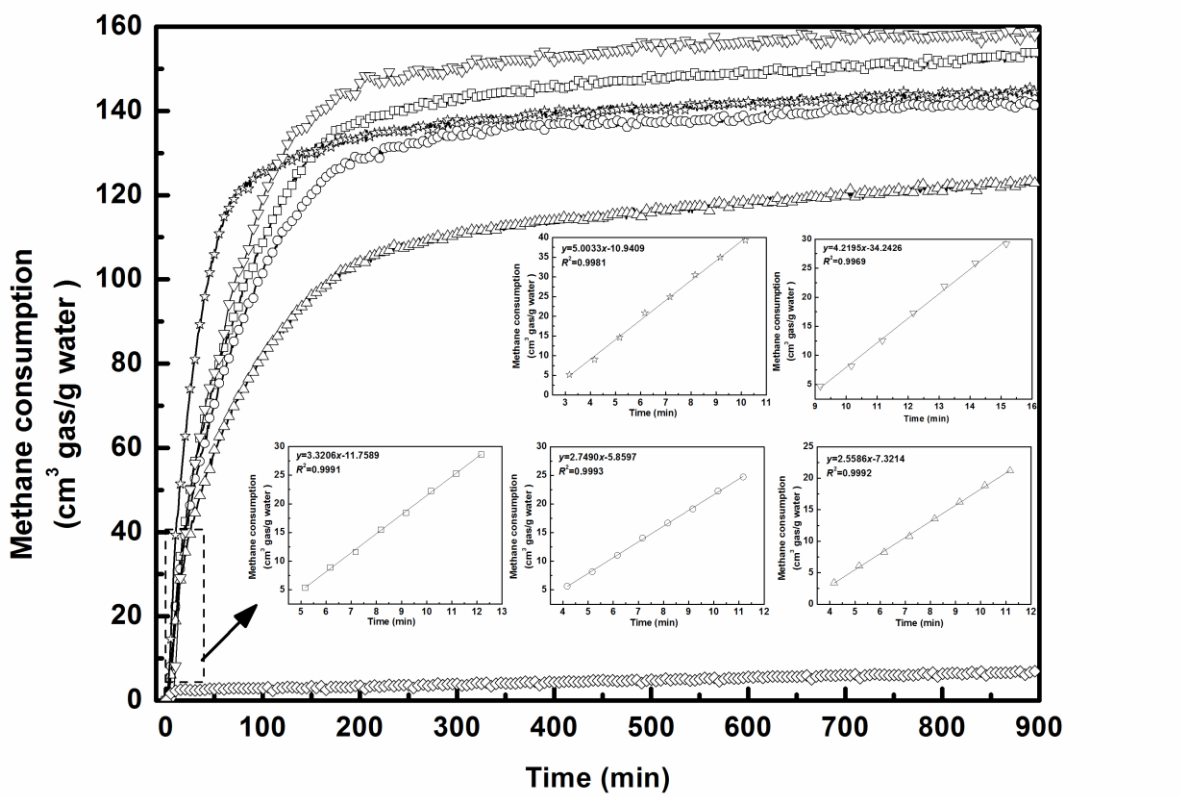

Figure 5 Consumption of methane by various hydrogel-dry water systems at various pressures: ▽dry water; □PHEMA (<100μm, 4.5MPa);○PHEMA-co-MAA (<100μm, 4.5MPa); △PHEMA-co-MAA (>100, 4.5 MPa), ☆ PHEMA-co-MAA (>100, 7.5 MPa) and ◇PHEMA (no silica, 4.5 MPa) (Operational conditions: T= 273.20K).

Table 1 Methane storage capacity in various systems.

Hydration System	**Methane Storage Capacity (cm^3/g water)**			
	Cycle 1 (***t_{90}, min**)	Cycle 2	Cycle 3	Cycle 4-8
DW	160 (172)	126	92	-
PHEMA or PHEMA-co-MAA	20-70 (-)**	-	-	-
DW+PHEMA (<100 μm, 4.5 MPa)	154 (210)	145	125	-
DW+PHEMA-co-MAA (<100 μm, 4.5 MPa)	141 (191)	126	121	-
DW+PHEMA-co-MAA (>100 μm, 4.5 MPa)	123 (293)	125	130	127-129
DW+PHEMA-co-MAA (<100 μm, 7.5 MPa)	144 (142)	117	110	-

*t_{90} is the time required for 90% methane hydrates to form within 900 min. ** poor reproducibility. No t_{90} was extracted from these data.

Methane hydrates formation in these mixtures was reversible. Shown in Figure 6 is the pressure-temperature plots of eight hydration cycles of methane gases when the mixed dry-water and PHEMA-co-MAA (>100 μm) was used at 4.5 MPa. The

calculated methane consumption was within the range of 123 cm^3/g and 129 cm^3/g, indicating an excellent reversibility.

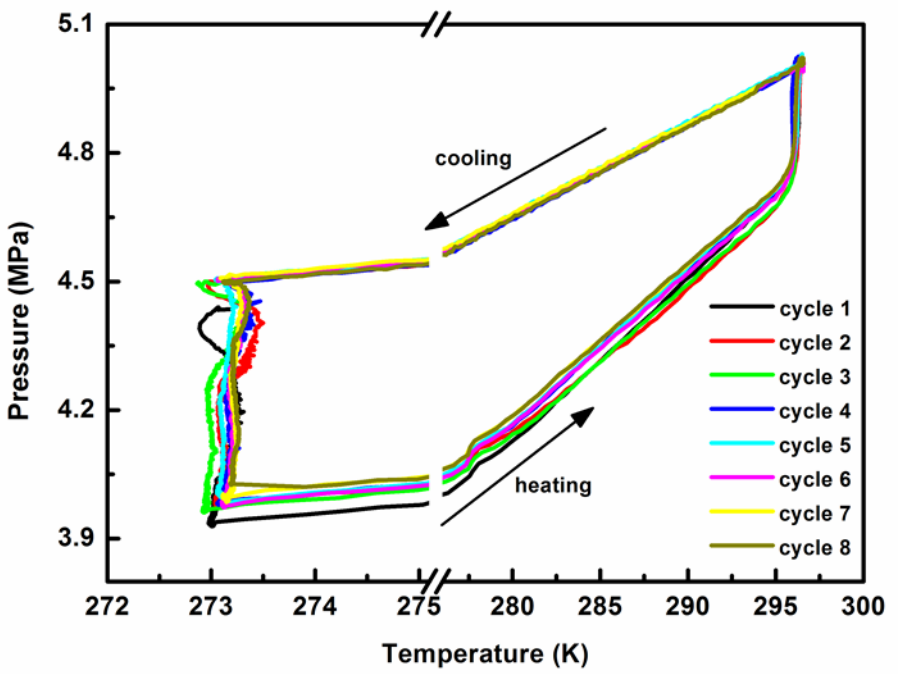

Figure 6 Reversed storage of methane in PHEMA-co-MAA (>100µm, 4.5 MPa, 8 cycles).

Same experiment was carried out using dry-water and the mixed dry-water and hydrogel particles for three cycles. The methane storage capacity of these systems was listed in Table 1. For dry water, the storage capacity reduced from 160 cm^3/g to 90 cm^3/g from cycle 1 to cycle 3, indicating its poor reusability. This is due to the destabilisation of dry-water as a consequence of the freeze-warm process as reported by Copper's group (Wang et al., 2008). When hydrogel particles were mixed with dry-water, the high methane capacity was well retained after three cycles (Table 1). The mixtures containing smaller hydrogels microspheres seemed less stable under higher pressure, although they have led to faster hydrates formation and greater methane storage capacity in a single storage experiment.

We hypothesized that the hydrogel particles and dry-water have stabilised each other in these mixed dry-water and hydrogel systems. The presence of hydrogel particles might not be able to prevent the coalescence of dry-water, as that of the gelling gel in Cooper's work (Carter et al., 2010). However, these particles absorb and retain the discharged water from 'dry water', and act alone as a hydration scaffold for the hydrates to form. Although the hydrogel particles alone are not tough/firm enough to stay unseparated and to act as a functional support for the hydrates formation, they can be stabilised by the dry water and/or the silica nanoparticles, therefore capable for effective hydration. This hypothesis is illustrated by Figure 7, in which hydrates first form from the initially mixed dry-water and hydrogel systems (Figure 7A). During the freeze-thaw process, the perfect structure of dry-water might be disrupted upon freezing, resulting in water discharged from it upon melting (Figure 7B). The free water is absorbed by the hydrogel particles at the same time and formation of hydrates in the mixture occurs upon cooling (Figure 6B'). With increased number of cycles, more and more water are freed out and the hydrogel particles become saturated (Figure 7C), leading to the system partially or fully covered by bulk volume of water. Therefore the formation of methane hydrates is retarred and methane capacity reduced. Without the presence of hydrogel particles, coalescence of the dry-water leads to a quick move of the process from A to C, methane hydration is irreversible. In the presence of hydrogel particles, reversible methane storage becomes possible. However the number of cycles changes depending on the operation condition as well as the size of hydrogel particles used. The water content also affects the capacity and reversibility of methane hydration which will be further investigated.

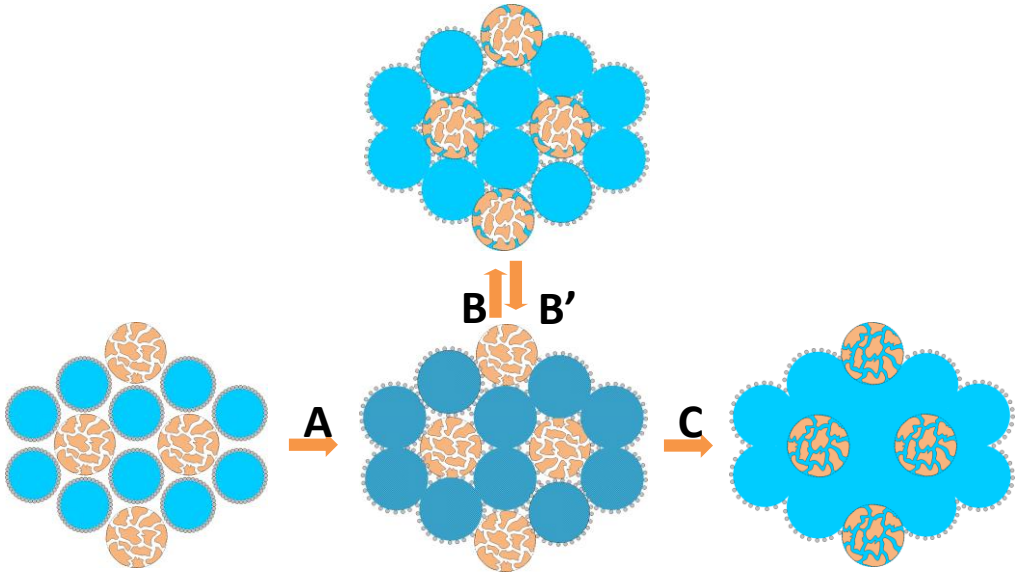

Figure 7 Illustration of reversible methane hydrates formation in a mixed dry-water and hydrogel system. A: the formation of methane hydrates in the mixed dry-water and hydrogel system; B: the thawing process leading to coalescence of dry-water; B': re-formation of hydrates from the thawed dry-water and hydrogel system; C: the formation of water saturated system that is unable or slow to re-hydrate with methane.

Conclusions

In summary, we have synthesised porous PHEMA and PHEMA-co-MAA hydrogel microspheres that results in systems capable of high capacity and reversible methane storage when mixed with dry-water. The excellent reversibility of the mixed colloidal systems is attributed to the co-stabilising effect between the hydrogel microspheres and the dry-water droplets. Increased operating pressure and smaller particle size enhance storage capacity and the formation kinetics, however reduce the stability, therefore the reusability of the systems. The hydrogel microspheres alone are too soft and adhesive to support the formation of methane hydrates. We are working on the materials to improve the rigidity so that the porous hydrogels alone can be used for reversible methane storage.

Acknowledgement

The authors wish to thank the Australia-China Natural Gas Technology Partnership Fund for financial assistance to this work.

References

Binks, B.P., Murakami, R., 2006. Phase inversion of particle-stabilized materials from foams to dry water. Nature Materials 5, 865–869.

Carter, B.O., Wang, W., Adams, D.J., Cooper, A.I., 2010. Gas storage in "dry water" and "dry gel" clathrates. Langmuir 26, 3186–3193.

Chirila, T.V., Hicks, C.R., Dalton, P.D., Vijayasekaran, S., Lou, X., Hong, Y., Clayton, A.B., Ziegelaar, B., Fitton. H., Platten, S., Crawford, G.J., Constable, I.J., 1998. Artificial cornea. Progress Polymer Science 23, 447- 473.

Giavarini, C., Maccioni, F., Santarelli, M.L., 2008. Dissociation rate of THF-methane hydrate. Petroleum Science and Technology 26, 2147–2158.

Gudmundsson, J.S., Graff O.F., 2003. Hydrate non-pipeline technology for transport of natural gas, in Proceedings of the 22nd World Gas Conference, Tokyo.

Hicks, C.R., Morrison, D., Lou, X., Crawford, G.J., Gadjatsy, A., Constable, I.J., 2006. Orbit implants: Potential new directions. Expert Rev Med Devices 3, 805-815.

Horak, D., Lednicky, F., Rehak, V., Svec, F., 1993. Porous polyHEMA beads prepared by suspension polymerization in aqueous medium. Journal of Applied Polymer Science 49, 2041–2050.

Horak, D., Adamyan, A., Golubeva, O., Skuba, N., Vinokurova, T., 2006. Poly(2-hydroxyethyl methacrylate) microspheres/liquid poly(dimethylsiloxane) composition for correction of small defects in face: histological evaluation in animal experiment. Journal of Materials Science: Materials in Medicine 17, 123–129.

Karaaslan, U., Parlaktuna, M., 2000. Surfactants as hydrate promoter?. Energy & Fuels 14, 1103–1107.

Koh, C.A., 2002. Towards a fundamental understanding of natural gas hydrates, Chemical Society Reviews 31, 157–167.

Lee, S.Y., Zhang, J.S., Mehta, R., Woo, T.K., Lee, J.W., 2007. Methane hydrate equilibrium and formation kinetics in the presence of an anionic surfactant. The Journal of Physical Chemistry C 111, 4734–4739.

Lou, X., Munro, S., Wang, S., 2004. Drug release characteristics of phase separation pHEMA sponge materials. Biomaterials 23, 5071–5080.

Lou, X., Wang, S., Tan, S.Y., 2007. Mathematics aided quantitative analysis of diffusion characteristics of pHEMA spongy hydrogels. Asia-Pacific Journal of Chemical Engineering 2, 609–617.

Masoudi, R., Tohidi, B., 2005. Gas hydrate production technology for natural gas storage and transportation and CO_2 sequestration. In: 14th SPE Middle East Oil and Gas Show and Conference, International Exhibition Centre, Bahrain.

Mori, Y.H., 2003. Recent advances in hydrate—based technologies for natural gas storage_a review. Journal of Chemical Industry and Engineering (China) 54(zl), 1-17.

Okutani, K., Kuwabara, Y., Mori, Y.H., 2008. Surfactant effects on hydrate formation in an unstirred gas/liquid system: An experimental study using methane and sodium alkyl sulfates. Chemical Engineering Science 63, 183–194.

Redlich, O., Kwong, J.N.S., 1949. On the thermodynamics of soloutions. V an equation of state, Fugacities of gaseous solutions. Chemical Reviews 44, 233–244.

Sloan, E.D., 2003. Fundamental principles and applications of natural gas hydrates. Nature 426, 353–359.

Sloan, E.D., Koh, C.A., 2008. Clathrate Hydrates of Natural Gases, 3rd edition. CRC Press/Taylor & Francis, Boca Raton, FL.

Stern, L.A., Circone, S., Kirby, S.H., Durham W. B., 2001. Anomalous Preservation of Pure Methane Hydrate at 1 atm. Journal of Physical Chemistry B 105, 1756-1762.

Su, F., Bray, C.L., Tan, B., Cooper, A.I., 2008. Rapid and reversible hydrogen storage in clatharate hydrates using emulsion-templated polymers. Advance Materials 20, 2663–2666.

Su, F., Bray, C.L., Carter, B.O., Overend, G., Cropper, C., Iggo, J.A., Khimyak, Y.Z., Fogg, A.M., Cooper, A.I., 2009. Reversible hydrogen storage in hydrogel clathrate hydrates. Advance Materials 21, 2382–2386.

Sun, Z.G., Wang, R.Z., Ma, R.S., Guo, K.H., Fan, S.S., 2003. Natural gas storage in hydrates with the presence of promoters. Energy Conversion and Management 44, 2733–2742.

Talyzin, A., 2008. Feasibility of H_2-THF-H_2O clathrate hydrate for hydrogen storage applications. International Journal of Hydrogen Energy 22, 111–115.

Wang, W., Bray, C.L., Adams, D.J., Cooper, A.I., 2008. Methane storage in dry water gas hydrates. Journal of the American Chemical Society 130, 11608–11609.

Wang, W., Carter, B.O., Bray, C.L., Steiner, A., Bacsa, J., Jones, J.T.A., Cropper, C., Khimyak, Y.Z., Adams, D.J., Cooper, A.I., 2009. Reversible methane storage in a polymer-supported semi-clathrate hydrate at ambient temperature and pressure. Chemistry of Materials 21, 3810–3815.

Wang, S., Mohd Mahali, S., McGuiness, A., Lou, X., 2010. Mathematical models for estimating effective diffusion parameters of spherical drug delivery devices. Theoretical Chemistry Account 125, 659-669.

Yang L., Fan, S.S., Wang, Y.H., Lang, X.M., Xie, D.L., 2011. Accelerated formation of methane hydrate in aluminum foam. Industrial & Engineering Chemistry Research 50, 11563–11569.

Yoslim, J., Linga, P., Englezos, P., 2010. Enhanced growth of methane–propane clathrate hydrate crystals with sodium dodecyl sulfate, sodium tetradecyl sulfate, and sodium hexadecyl sulfate surfactants. Journal of Crystal Growth 313, 68–80.

Zhang, C.S., Fan, S.S., Liang, D.Q., Guo, K.H., 2004. Effect of additives on formation of natural gas hydrate. Fuel 83, 2115–2121.

Zhong, Y., Rogers, R.E., 2000. Surfactant effects on gas hydrate formation. Chemical Engineering Science 55, 4175–4187.